Magnetic properties of ferromagnet-antiferromagnet superlattice structures with mixed-spin antiferromagnetic sheets

L. L. Hinchey and D. L. Mills
Department of Physics, University of California, Irvine, California 92717
(Received 3 March 1986)

We present theoretical studies of the properties of superlattices constructed by alternating films of ferromagnetic and antiferromagnetic materials, each described through use of a localized spin model. The interface between the ferromagnetic and antiferromagnetic constituents is a (110) surface of a bcc lattice. For this system, this geometry places mixed-spin antiferromagnetic sheets adjacent to the ferromagnetic films. The study of the classical ground state as a function of external magnetic field shows that in zero field the ground state has spins canted to minimize total exchange energy at the interface. We find that a different sequence of magnetic-field-induced spin-reorientation transitions occur for various values of the interface exchange constant. For the various phases, we present calculations of the spin-wave spectrum and the infrared absorption spectrum of the superlattice structure.

I. INTRODUCTION

During the past decade there has been considerable interest in the synthesis and study of superlattices found from alternating layers of different materials. Superlattices of excellent quality have been formed from semiconducting materials. In these samples, the interfaces between adjacent media are perfectly sharp on the atomic scale. The quality of the interfaces in superlattices constructed from magnetic materials is inferior to that realized with semiconductors at present. However, there is an older literature on magnetic multilayer systems, for example Co-Cr superlattices[1] and multilayer systems formed from Mn-Fe and Permalloy,[2,3] and sample quality is improving steadily. Quite recently, very high quality Y-Gd superlattices have appeared.[4] These may be synthesized with very thin films, and interfaces of high quality, approaching that realized in the semiconducting superlattices. Interest in such composite materials arises because one may create new materials in the laboratory, with properties distinct from those of any one constituent.

In this paper, we continue our theoretical study of superlattices constructed from magnetic materials. As we have shown in our previous work,[5,6] such systems have intriguing macroscopic physical properties which are influenced strongly by the microscopic details of the underlying superlattice. For example, one can construct materials with microwave or infrared response characteristics subject to design. We have also shown for certain geometries, that magnetic-field-induced spin-reorientation transitions may occur for externally applied magnetic fields of modest magnitudes.

In magnetic superlattices, elementary excitations such as spin waves are collective excitations of the structure as a whole, and as a consequence have properties distinctly different from the modes associated with any one constituent. Collective excitations in magnetic superlattices fabricated from alternating layers of Ni and Mo have been studied experimentally.[7] Damon-Eshbach[8] surface spin waves on the individual Ni films may interact in the long-wavelength limit through dipole fields generated by the spin motion, to form collective excitations which transmit energy normal to the interfaces between the films.[9–11] Our calculations[5,6] for superlattices formed by alternating layers of ferromagnetic and antiferromagnetic materials outline the properties of spin-wave excitations, in the short-wavelength limit, where exchange couplings provide the dominant contribution to the excitation energy.

A rich variety of behaviors may be expected if one forms superlattices by alternating ferromagnetic and antiferromagnetic films. Consider the case (the only geometry considered in this paper) where the antiferromagnetic constituent consists of sheets of spin within which there is antiferromagnetic alignment of the moments. This configuration is realized for bcc materials, when the interface between the ferromagnet and antiferromagnet is along the [110] direction. We refer to this structure as a (110) superlattice. In our previous work we considered a similar bcc system, referred to in this paper as a (100) superlattice, in which the interface between the ferromagnet and antiferromagnet is a (100) surface. In the (100) systems, the antiferromagnet consists of sheets of spin within which the moments are aligned ferromagnetically. We show the ground state of the (110) superlattice in zero external magnetic field in Fig. 1(a), in the limit that the interface exchange constant is zero. The length of the unit cell is d_1+d_2, and there are two spins per sheet of spins in the unit cell. We show a detailed view of the interface in Fig. 1(b). When the interface coupling is "turned on" we expect rearrangement of the interface spins. From the point of view of the ferromagnet, this rearrangement relieves the torque on those up ferromagnetic spins with down antiferromagnetic nearest neighbors (assuming the interface coupling is ferromagnetic in sign).

As we shall see, the (110) superlattice is a system in which the ferromagnet and the antiferromagnet are in a spin-canted state in zero external magnetic field. When a

variable magnetic field is applied, a series of spin-reorientation transitions occurs. The phase diagram is particularly complex for the case when the interface exchange constant is smaller, by a specific amount, than the exchange constant within the ferromagnet. The fields required to induce these transitions are small compared to the bulk antiferromagnet spin-flop field. Furthermore, these transition fields are subject to control through appropriate design of the superlattice structure.

Section II of this paper explores the field dependence of the ground-state spin configuration for superlattices such as that in Fig. 1, all of infinite extent, in which the antiferromagnetic constituent consists of sheets of spin each with antiferromagnetic alignment of the moments. We use a localized spin model, with nearest-neighbor exchange interactions of appropriate sign in each material, as the basis of our calculation.[12] The sign of the exchange interaction across the interface between ferromagnet and antiferromagnet does not affect the behavior of these structures. We include uniaxial anisotropy in the antiferromagnetic medium. In Sec. III we discuss the spin-wave spectrum of the superlattice structure, for the various ground-state spin patterns examined in Sec. II. As was the case for the (100) superlattice discussed in a previous paper,[6] a subset of the modes are collective excitations of the entire superlattice system, while others are confined nearly exclusively to one constituent, with character similar to the standing-wave spin resonances of thin films. A new feature is the localization of a number of modes to the first several interface layers of each constituent. In Sec. IV we present studies of the magnetic field variation of the microwave and infrared absorption spectrum.

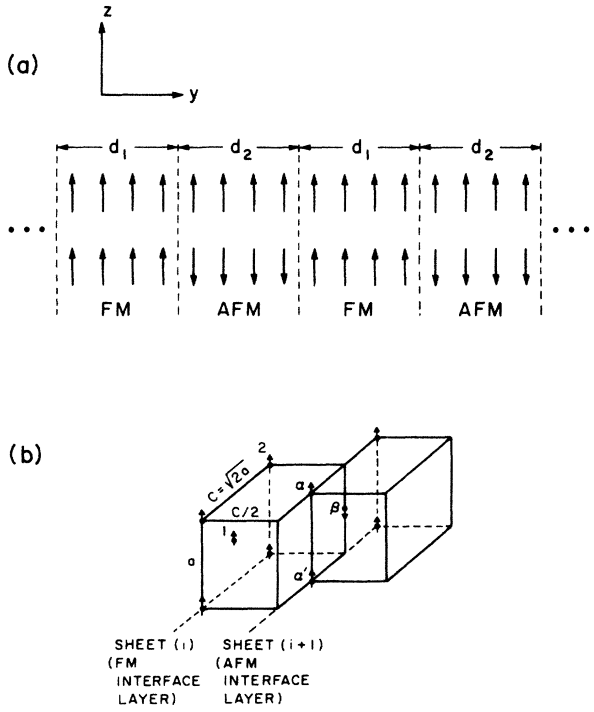

FIG. 1. (a) For the superlattice geometry of interest in the present paper, we show the zero-field ground-state in the limit that the interface exchange coupling between ferromagnet and antiferromagnet is zero. The length of the unit cell is d_1+d_2, and there are two spins in the unit cell. (b) We show a detailed view of the interface between the ferromagnetic and antiferromagnetic films. The crystal structure is body-centered cubic with edge length $l=a$ (the diagram is not to scale). The interface is a (110) plane, and a given ferromagnetic interface spin is exchange coupled to six ferromagnetic spins (four are in the same sheet as the spin of interest), and two antiferromagnetic spins. The two antiferromagnetic nearest neighbors of spin 1 (in the ferromagnetic sheet) are labeled α and α', and the illustrated antiferromagnetic nearest neighbor of spin 2 is labeled β.

II. DETERMINATION OF THE CLASSICAL GROUND STATE OF THE SUPERLATTICE: THE PHASE DIAGRAM AT ZERO TEMPERATURE

As discussed in Sec. I, we study a superlattice that consists of ferromagnetic films each with $N_{\rm FM}$ layers, and antiferromagnetic films each with $N_{\rm AFM}$ layers. Each is a bcc lattice of spins with the same lattice constant, and each site is occupied by a localized spin S, which we assume is the same for the ferromagnet (FM) and antiferromagnet (AFM). This assumption simply serves to limit the number of parameters in our model. The interface between ferromagnet and antiferromagnet is a (110) surface. We have nearest-neighbor exchange interactions of strength $J_{\rm FM}$ within the ferromagnet, $J_{\rm AFM}$ within the antiferromagnet, and J_I across the interface. In addition, within the antiferromagnet we have uniaxial, single-site anisotropy of the form KS_z^2.

As remarked earlier, antiferromagnetic constituent of a superlattice with this geometry consists of mixed-spin sheets of spins, within which there is antiferromagnetic alignment of the moments. In the limit that the interface exchange constant $J_I=0$, the spin directions are parallel to the (110) plane for the case where the easy axis lies within this plane.[12] Since there are an equal number of alternating up and down antiferromagnetic spins adjacent to the ferromagnet interface layers, we expect the spins at the interface to relax from their positions in Fig. 1(a), along the $+\hat{\mathbf{z}}$ and $-\hat{\mathbf{z}}$ directions, to a spin-flop configuration when $J_I\neq 0$, even in zero external field. In essence, the ferromagnetic spins exert a strong exchange field on the antiferromagnetic spins closest to the interface, and provoke such an instability. We will say more about this later.

We now proceed to determine the ground-state spin configuration of the ferromagnetic-antiferromagnet superlattice with (110) interfaces, for two values of the interface coupling constant J_I. We then discuss the magnetic field variation of the ground-state spin configuration, and construct a phase diagram of the system (at $T=0$) for both values of J_I.

To begin, we must choose a set of parameters for the numerical analysis. We mention here that for the present case the ground-state spin arrangement of the superlattice does not depend on whether the number $N_{\rm AFM}$ of planes in the antiferromagnet is even or odd, because each plane in the antiferromagnet contains an equal number of up

and down spins.[13] The antiferromagnet is characterized by the exchange field $H_E = zJ_{\rm AFM}S$ and the anisotropy field $H_A = 2KS$, where K is the anisotropy constant in the single-ion anisotropy term KS_z^2, present for each spin. For this description of the anisotropy field, we consider classical spins (large S), and thus ignore the distinction between $2KS$ and $2K(S-\frac{1}{2})$. We choose $H_A/H_E = 0.05$, a value characteristic of MnF_2, a classical antiferromagnet with modest anisotropy. We have no specific magnetic materials in mind for the ferromagnetic constituent. We choose the exchange constant $J_{\rm FM}$ in the ferromagnet to be equal to that in the antiferromagnet, and the spins S are also taken equal as remarked earlier. We have chosen two values for the interface exchange constant J_I: (1) $J_I = \frac{3}{2}J_{\rm FM} = \frac{3}{2}J_{\rm AFM}$ and (2) $J_I = \frac{1}{2}J_{\rm FM} = \frac{1}{2}J_{\rm AFM}$.

When the value of the interface exchange constant J_I satisfies the condition $J_I < 0.79J_{\rm FM}$ [as it does in case (2) above], we find that exchange and anisotropy energies within the antiferromagnet overwhelm the interface exchange energy even when the antiferromagnetic films are quite thin, and a consequence is that the magnetic field dependence of the ground-state spin configuration is complex. We find four distinctly different phases here, with a complex arrangement in the phase diagram, for case (2) when $J_I = 0.5$, and only three phases for case (1) when $J_I = 1.5$ (for $J_{\rm FM} = J_{\rm AFM} = 1$). This is for a superlattice formed from antiferromagnetic films four layers thick. We see that in the present case, the strength of the interfacial coupling controls the phase diagram strongly.

As described in Sec. I, the unit cell of the structure has length $d_1 + d_2$. Then the number of planes of spin in the unit cell is $N_{\rm FM} + N_{\rm AFM}$. We break each sheet up into unit cells, each of which contain two spins. In the antiferromagnet it is clear this must be done, and we use the same scheme in the ferromagnetic film because half the ferromagnetic spins (i) at the interface are adjacent to up antiferromagnetic spins, while the remaining ferromagnetic spins (i') are adjacent to down antiferromagnetic spins, before the spins are allowed to relax. After relaxation, spins i and i' in sheet i may not have the same angle with respect to the z axis even in the ferromagnet, as a consequence of exchange coupling across the interface. We allow the spins labeled i in a given sheet to rotate away from the z axis by the angle θ_i, and those labeled i' to rotate by angle θ_i', always confined to the xz plane.[14] The spin configuration is thus described by this set of $2(N_{\rm FM} + N_{\rm AFM})$ angles. The object is to find the set of angles which minimizes the energy of the spin system. We do this by an iterative procedure, in which we rotate each spin into its local effective field. We begin with an arbitrarily chosen set of angles. For each spin, we calculate the local field generated by the spins in neighboring planes, and that associated with the single-site anisotropy energy KS_z^2. We then rotate each spin into its local field, a step guaranteed to lower the energy of the system. We continue until we achieve a configuration in which each spin is aligned with the effective field, and we achieve a set of angles $\{\tilde{\theta},\tilde{\theta}'\}$ which satisfy the set of energy minimization equations generated by the criterion $\partial(E\{\theta_j\})/\partial\theta_i = 0$. For the set of angles $\{\tilde{\theta}\}$, the energy minimization condition is

$$\tan\tilde{\theta}_i = \frac{H_x^{(i)} - 2KS\sin\theta_i}{H_z^{(i)}} , \tag{2.1}$$

where

$$H_x^{(i)} = S(2J_{i-1}\sin\theta'_{i-1} + 4J_i\sin\theta'_i + 2J_{i+1}\sin\theta'_{i+1}) ,$$
$$H_z^{(i)} = S(2J_{i-1}\cos\theta'_{i-1} + 4J_i\cos\theta'_i + 2J_{i+1}\cos\theta'_{i+1}) + H_0 , \tag{2.2}$$

with J_i defined as the exchange-coupling strength between nearest neighbors in the same spin sheet. To find the set of angles $\{\tilde{\theta}'\}$, we simply interchange the positions of θ and θ' in the equations above.

We show the ground-state spin configurations resulting from this calculation, for various values of the Zeeman field H_0, in Fig. 2 for $J_I = 0.5$ and Fig. 3 for $J_I = 1.5$. Each circle represents the projection of a spin in the xz plane, and there are two spins illustrated per sheet. The orientations of the spins in each sheet are indicated by arrows. In the absence of an external magnetic field (neglecting dipolar fields), the spins in the ferromagnetic sheets are canted at $\theta \simeq 90°$ to minimize total exchange energy due to interaction with the mixed-spin antiferromagnetic sheets. As we see from Fig. 1(b), each interface ferromagnetic spin is exchange coupled to either two up-spin

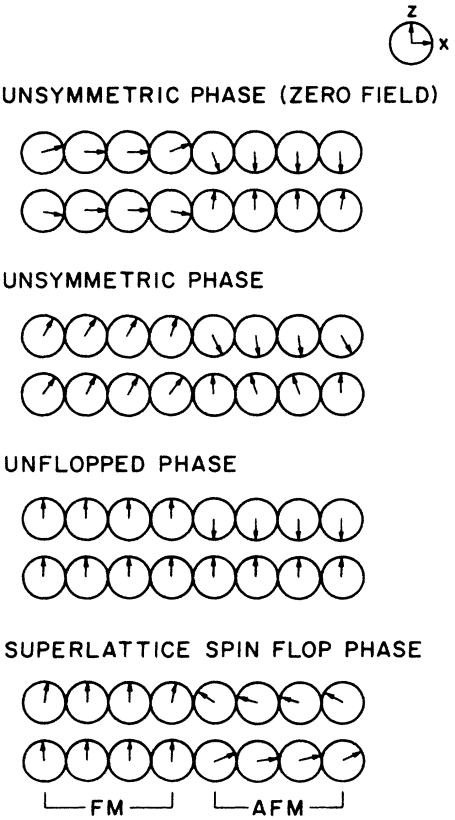

FIG. 2. For $N_{\rm FM} = N_{\rm AFM} = 4$ and $J_I = 0.5$, we show the spin arrangement in (a) the unsymmetric phase when $H_0 = 0$, (b) the unsymmetric phase when $H_0 = 0.04$, (c) the unflopped phase, and (d) the superlattice spin-flop phase when $H_0 = 0.78$. Each circle lies in the xz plane, and the two arrows per plane indicate the orientation of the two subsets of spins in a given plane. Here and elsewhere in the paper, the magnetic fields are measured in units of $(2H_EH_A)^{1/2}$.

or two down-spin antiferromagnetic spins (in addition to six ferromagnetic spins). The minimum energy configuration for two adjacent interface ferromagnetic spins, one coupled to up antiferromagnetic spins and the other coupled to down antiferromagnetic spins, occurs when both ferromagnetic spins are canted at $\theta=90°$. The canted ferromagnetic spins exert an exchange torque on the antiferromagnetic interface spins, causing the antiferromagnetic spins near the interface to twist away from the z axis. The resulting torque on the ferromagnet drives the ferromagnetic interface spins away from $\theta=90°$ exactly.

At this point it is useful to recall the phase diagram of the bulk antiferromagnet at $T=0$. As H_0 is increased from zero, one encounters the first-order spin-flop transition at the lower critical field of $(2H_EH_A)^{1/2}$ when $H_E \gg H_A$.[15] The spins are canted at angles $\pm\theta$ from their original spin axis. As H_0 is increased, the spins on each sublattice rotate into the field H_0, until a second critical field is reached where they are aligned fully with the field. At the point where the spins just align, one has a second-order phase transition. The high-field phase is referred to as the paramagnetic phase.

Clearly, for the superlattice, when H_0 is so large that both exchange and anisotropy energies are overwhelmed by the Zeeman energy, we shall realize an analogue of the paramagnetic phase, with all spins fully aligned along H_0. We find three distinctly different phases below the paramagnetic phase, for the case when $J_I=0.5$, and two phases below the paramagnetic phase when $J_I=1.5$.

The phase diagram of the superlattice is given in Fig. 4(a), for the case when $J_I=0.5$. We take $N_{\rm FM}=N_{\rm AFM}$ al-

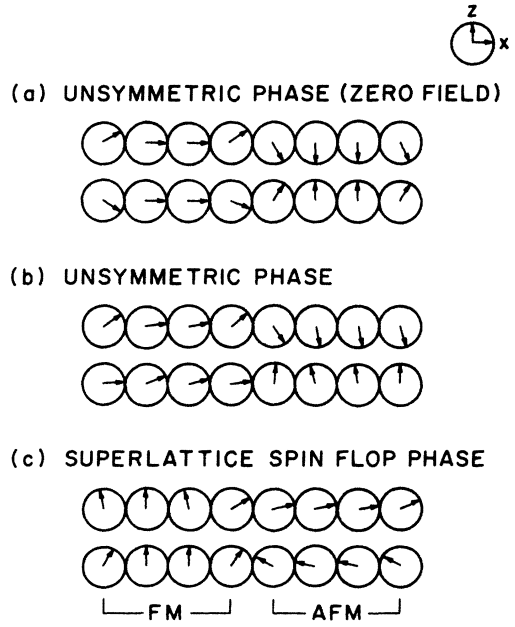

FIG. 3. For $N_{\rm FM}=N_{\rm AFM}=4$ and $J_I=1.5$, we show the spin arrangement in (a) the unsymmetric phase when $H_0=0$, (b) the unsymmetric phase when $H_0=0.04$, and (c) the superlattice spin-flop phase when $H_0=0.78$. Each circle lies in the xz plane, and the two arrows per plane indicate the orientation of each subset of spins in a given plane.

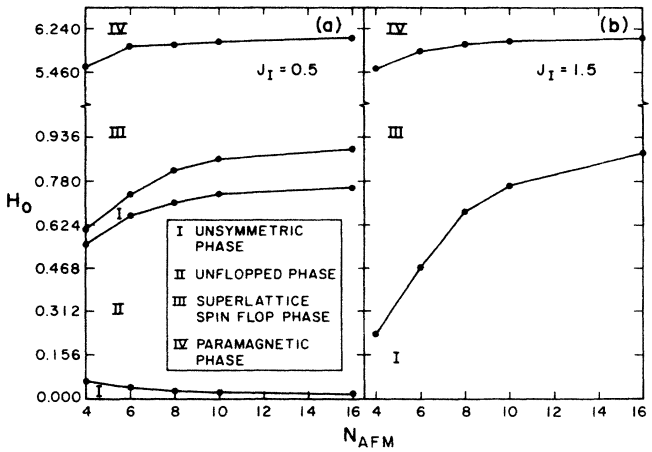

FIG. 4. For the case $N_{\rm FM}=N_{\rm AFM}$, when $N_{\rm AFM}$ ranges from 4 to 16, we plot the critical fields required for the various phase transitions discussed in the main text for (a) $J_I=0.5$, and (b) $J_I=1.5$. For comparison, the bulk antiferromagnet enters the spin-flop phase at the critical field $H_c^{(1)}=1.0$ (in the same reduced units in the figure), and enters the paramagnetic phase at $H_c^{(2)}=6.2$ (in reduced units).

ways, with $N_{\rm FM}$ ranging from 4 to 16. As remarked above, the first low-field phase is a spin-flop state, which we refer to simply as the unsymmetric state. This state results when the antiferromagnetic spins on the down-spin sublattice twist away from the $-z$ direction by angles *larger* than those by which the spins on the up-spin sublattice twist away from the $+z$ direction. The spins at the interface suffer the greatest flopping angles, as illustrated in Fig. 2(b), by a spin configuration corresponding to the unsymmetric state. This exchange-energy induced twist is resisted by the antiferromagnetic film since we are well below the reduced bulk antiferromagnetic spin-flop field $H_0=1.0$.

As the Zeeman field is raised, we encounter a second-order phase transition to a pure unflopped phase. The spin configuration of this phase is illustrated in Fig. 2(c); all spins are aligned parallel to or antiparallel to the $\hat{z}$ axis. The unflopped configuration of the antiferromagnet results when the exchange and anisotropy energies within the ferromagnet overwhelm the interface exchange energy. In terms of the parameters used in this paper, the condition on the interface exchange constant, which allows the unflopped state to exist, is $J_I \leq 0.79 J_{\rm FM}$ when $J_{\rm FM}=J_{\rm AFM}$ and $N_{\rm FM}=N_{\rm AFM}=4$.

Increasing the field induces a second-order transition back to the unsymmetric state. As the Zeeman field is raised further, the superlattice undergoes another second-order phase transition to a highly symmetric phase we call the superlattice spin-flop state. In this phase the spin configuration of the primed spins in a given sheet is obtained from that of the unprimed spins in the same sheet by a reflection through the yz plane (i.e., $\theta_i'=-\theta_i$). In this phase the unit cell has zero net transverse moment. Since we are at field strengths which range from just below to above the reduced bulk antiferromagnet spin-flop field $H_c=1.0$, we find large spin-flop angles throughout the

antiferromagnetic film. The spins in the ferromagnet, however, are nearly aligned along the direction of the field. When we study the spin-wave spectrum of the superlattice in the superlattice spin-flop state in Sec. III, we shall find that this unequal distribution of spin deviation will have a pronounced effect on the dispersion relation of the lowest frequency mode of the system. As we shall also see in the next section, the transition from the unsymmetric state to the superlattice spin-flop state is characterized by the softening of one of the superlattice spin modes. A spin configuration corresponding to the superlattice spin-flop state is given in Fig. 2(d).

Finally, at high fields, the superlattice exists in the fully-aligned paramagnetic phase similar in nature to that in the bulk antiferromagnet. The transition from the superlattice spin-flop state to the paramagnetic state is second order, as in bulk antiferromagnets.

When J_I takes on a value greater than $0.79J_{\rm FM}$, the phase diagram of the superlattice is greatly simplified. In Fig. 4(b), we show the phase diagram of the superlattice when $J_I=1.5J_{\rm FM}$. Because J_I is greater than the critical value, as described previously, we do not realize the pure unflopped state for this system.

Again, the first low-field phase is the unsymmetric phase. Because there is now greater exchange energy associated with the interface spins, the spin-flop angles at the interface are greater than those for the case when $J_I=0.5$ [see Fig. 3(b)]. When the magnetic field is increased, we encounter a second-order transition directly to the superlattice spin-flop state, followed by another second-order transition to the paramagnetic state. This behavior is analogous to that of the (100) superlattice discussed in an earlier paper,[6] with the exception that now the low-field phase is a spin-flop state, instead of an unflopped state.

There is no hysteresis in the superlattice transitions as there is at the bulk antiferromagnet phase transition (antiferromagnetic state $\rightarrow$ spin-flop state), since the superlattice phase transitions are second order in character.

III. THE SPIN-WAVE EXCITATIONS OF THE SUPERLATTICE STRUCTURE

In this section, we analyze the spin-wave spectrum of the superlattice structure. We have carried out detailed studies of the elementary excitations as a function of the externally applied Zeeman field H_0, as the field is swept through the phase diagrams in Fig. 4.

The formalism we have used in this study is not described in detail in this paper. For a complete discussion, see our paper[6] on the (100) superlattice, Appendix A. We present here only a brief description of the formalism used to calculate the spin-wave spectrum. Recall that our unit cell contains two spins, i and i', per sheet or spins in the superlattice structure, canted away from the z axis by angles θ_i and θ_i' respectively. If $l=l_x,l_y,l_z$ denotes the site of a particular spin, with the y axis normal to the interfaces in the superlattice structure, the spin at this site is canted away from the z axis by the angle θ_{l_y}, with the spin in the xz plane. Similarly, if $l'=l_x',l_y,l_z'$ denotes the site of the second spin of the sheet at l_y, the spin at this site is canted away from the z axis by the angle θ_{l_y}', again with the spin in the xz plane. We erect a new coordinate system $x'y'z'$ at site l and $x''y''z''$ at site l', with the z' axis parallel to the spin at l and the z'' axis parallel to the spin at l'. The $x'z'$ plane and the $x''z''$ plane are parallel to the old xz plane. We then obtain linearized equations of motion for the operators

$$S'_{\pm}(l)=S_{x'}(l)\pm iS_{y'}(l)$$

and

$$S''_{\pm}(l')=S_{x''}(l')\pm iS_{y''}(l')\ ,$$

which describe the spin deviations away from the z' axis and the z'' axis, respectively. The linearized equations of motion for $S'_{\pm}(l)$, where $S'_{\pm}(l)$ have the time dependence $\exp(-i\Omega t)$, are given below:

$$\begin{aligned}\pm\Omega S'_{\pm}(l)=&S\sum_{\delta}J(l,l,+\delta)\{A(l,l+\delta)S'_{\pm}(l)-\tfrac{1}{2}[A(l,l+\delta)+1]S'_{\pm}(l+\delta)\}\\&-\tfrac{1}{2}S\sum_{\sigma}J(l,l+\delta)[A(l,l+\delta)-1]S'_{\mp}(l+\delta)+H_0S'_{\pm}(l)\cos\theta_l\\&+[KSS'_{\pm}(l)(2\cos^2\theta_l-\sin^2\theta_l)-KSS'_{\mp}(l)\sin^2\theta_l]\delta_{l,l_{\rm AFM}}\ ,\end{aligned}\tag{3.1}$$

where

$$A(l,l,+\delta)=(\cos\theta_l\cos\theta_{l+\delta}+\sin\theta_l\sin\theta_{l+\delta})\ .$$

The sum over δ ranges over nearest neighbors.

Since the transformation described above does not destroy translational invariance in the x and z directions, for each subset of spins in a given sheet, we may apply periodic boundary conditions in these two coordinates. Thus, we have solutions of the Bloch form,

$$S'_{\pm}(l_xl_yl_z)=e^{ik_xl_x}e^{ik_zl_z}\mathcal{S}_{\pm}(l_y)\ .\tag{3.2}$$

The superlattice is also periodic in the y direction, and in the case of interest the superlattice unit cell consists of $(N_F+N_{\rm AFM})$ layers of spins. Thus, if l_y' and l_y refer to equivalent layers of spins in different superlattice unit cells, the solutions also have Bloch character in the y direction:

$$\mathcal{S}_{\pm}(l_y')=e^{ik_{\perp}(l_y'-l_y)}\mathcal{S}_{\pm}(l_y)\ .\tag{3.3}$$

By using Eq. (3.1) for all sites l and l', we are led to an eigenvalue equation for frequency Ω with the form

$$\pm\Omega S'_{\pm}(l)-\sum_{l'}[M_1(l,l')S'_{\pm}(l)+M_2(l,l')S'_{\mp}(l)]=0\ ,\tag{3.4}$$

where the explicit form of the matrices M_1 and M_2 can be constructed from Eq. (3.1). By taking advantage of the Bloch character of the solutions, given in Eqs. (3.2) and (3.3), the problem of calculating the spin-wave spectrum can be reduced to diagonalizing a $4(N_{\rm FM}+N_{\rm AFM})$-dimensional matrix. In general, in the canted states, the variable $\mathcal{S}_+(l_y)$ is coupled to $\mathcal{S}_-(l_y)$, so the spin precession is elliptical in nature. For each choice of k_x, k_z, and $k_\perp$ we then have $4(N_{\rm FM}+N_{\rm AFM})$ spin-wave frequencies, half of which are positive and half of which are negative. The excitation energy of a given mode is the absolute value of its frequency $\Omega_\alpha(\mathbf{k})$, where $\mathbf{k}=k_x\hat{\mathbf{x}}+k_y\hat{\mathbf{y}}+k_z\hat{\mathbf{z}}$.

We then have, upon diagonalizing the matrix just described, $4(N_{\rm FM}+N_{\rm AFM})$ spin-wave branches, each a function of $k_\perp$. A number of the modes have the character of standing-wave resonances of one of the two constituents media; in general, there is also appreciable amplitude for spin motions in the first layer of spins in the adjacent media. The behavior of the two or three lowest branches is particularly rich, since as the magnetic field is varied, we encounter regimes where we have collective motions of the entire superlattice, and regimes where the excitation is localized within the antiferromagnet. Thus, the discussion below focuses on these low-lying branches.

We begin our discussion with the spin-wave spectrum of the low-field ground states illustrated for a particular value of magnetic field in Figs. 2(b) and 3(b), for $J_I=0.5$ and 1.5, respectively. We shall then examine the behavior of the lowest-frequency spin-wave branch, as the magnetic field is swept through the various phases of the superlattice structure. In the interest of brevity, we only summarize the principle features here.

In Fig. 5 we show the three lowest positive-frequency spin-wave branches, for propagation normal to the interface, for a value of the magnetic field H_0 low enough to place both systems in the low-field unsymmetric state. The calculations are for $N_{\rm FM}=N_{\rm AFM}=4$. In the unsymmetric spin-flop state, the lowest branch of each structure has a frequency which vanishes with wave vector as $k_\perp\to 0$. This is the Goldstone mode of the system, which has vanishing frequency as $k_\perp\to 0$ by virtue of the fact that one may continuously rotate the spin about the z axis without affecting the energy of the system. (The existence of this symmetry operation depends on the fact that we have ignored dipolar interactions in the present system.) It follows that this low-frequency branch is in fact a collective mode of the superlattice structure as a whole, rather than an eigenmode localized to one or the other constituent. As we shall see, however, when the ferromagnetic spins are nearly aligned with the z axis, as they are in the superlattice spin-flop state, the Goldstone mode is *essentially* localized to the spin-flopped antiferromagnet with the consequence that the magnitude of this dispersion drops to zero.

The magnitude of the dispersion of the spin-wave branches is sensitive to the interfacial coupling strength between the ferromagnetic film and the antiferromagnetic film. At low fields, the spin-flop angles at the interface are larger for the larger value of J_I examined here ($J_I=1.5$), and consequently, the disturbance propagates farther into the adjacent media. Because strong coupling across the interface delocalizes the spin-wave disturbance, it leads to an increase in the magnitude of the dispersion. This effect may be observed for each mode in Fig. 5.

We pause at this point to recall properties of spin waves of the corresponding (100) superlattice (i.e., $N_{\rm FM}=N_{\rm AFM}=4$, $J_I=1.5$). In the low-field unflopped state, all modes show very little dispersion due to the alternating direction of the magnetic moment in the ferromagnetic films. In this system the spin waves have the character of standing-wave resonances of the individual constituents. Only when the Zeeman field is large enough to drive the system into the unsymmetric spin-flop state, with its several delocalized modes, do the eigenfrequencies of the of the structure show appreciable dispersion. In contrast, the (110) superlattice discussed in this paper has a number of delocalized modes, even in zero external field, which show appreciable dispersion. We shall see an analogue of the standing-wave resonances when we examine the behavior of the spin waves in the high-field unflopped phase of the (110) superlattice.

In Fig. 6 we show the lowest-frequency positive-spin-wave branch for the various phases of the superlattice, for $J_I=0.5$ (a)–(d) and $J_I=1.5$ (e) and (f), when $N_{\rm FM}=N_{\rm AFM}=4$. First we consider the case when $J_I=0.5$.

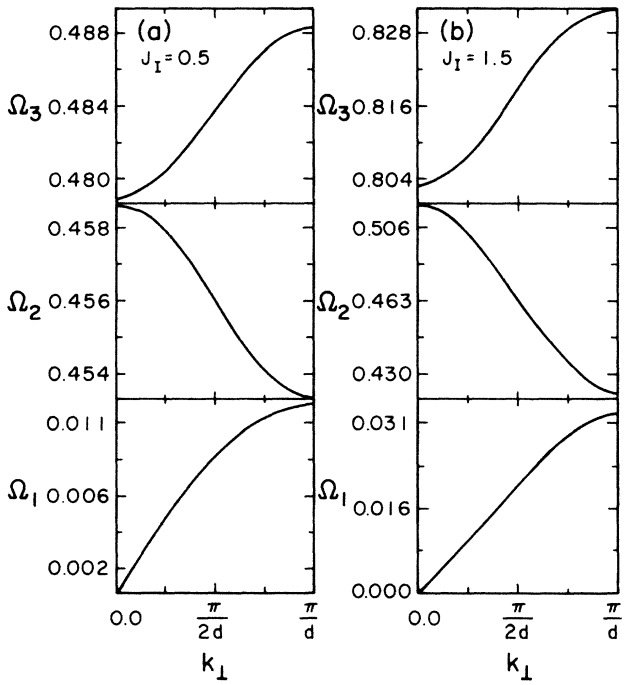

FIG. 5. For $k_x=k_z=0$, we show the dispersion relations of the three lowest-frequency positive spin-wave branches of the superlattice structure. The wave vector $k_\perp$ normal to the interfaces ranges through the superlattice Brillouin zone. The calculations assume the external field is small, $H_0=0.04$. The two cases considered are (a) $N_{\rm FM}=N_{\rm AFM}=4$ and $J_I=0.5$, where the ground state is that illustrated in Fig. 2(b), and (b) $N_{\rm FM}=N_{\rm AFM}=4$ and $J_I=1.5$, where the ground state is that illustrated in Fig. 3(b). The units of frequency are such that in the bulk antiferromagnet, the zero-field antiferromagnetic resonance frequency is unity.

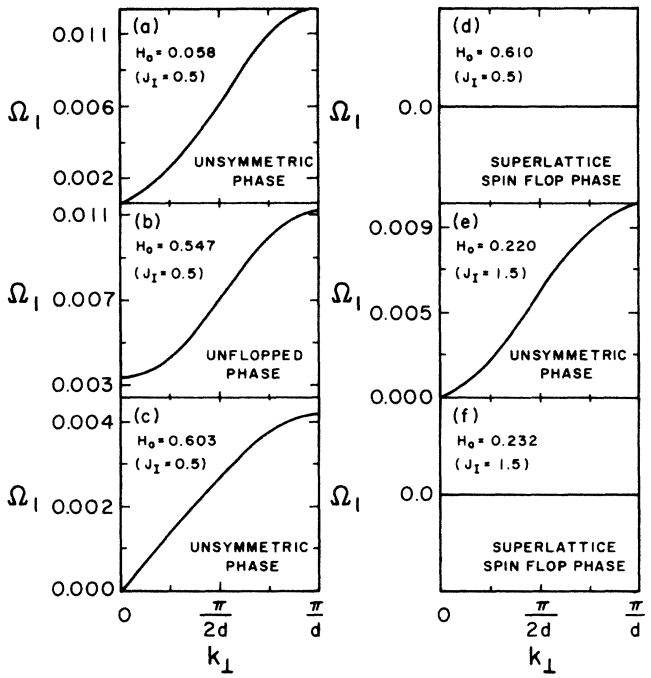

FIG. 6. We show the lowest positive frequency spin-wave branch of the superlattice when $J_I=0.5$ (a)–(d), and when $J_I=1.5$ (e) and (f), for various values of the Zeeman field H_0. Again the calculations are for $N_{\rm FM}=N_{\rm AFM}=4$.

In Fig. 6(a) we show the Goldstone mode in the unsymmetric spin-flop state, for a value of the field just below that required to drive the system into the unflopped state. The Goldstone mode still has a frequency which vanishes with wave vector as $k_\perp \to 0$, as symmetry requires; however, it exhibits much stronger curvature, for relatively small values of $k_\perp$, than we observe when the system is deep in the low-field unsymmetric state [cf. Ω_I in Fig. 5(a)]. Upon entry into the unflopped state, the rotational degree of freedom about the z axis disappears. As a consequence, the lowest-frequency positive mode now has nonzero frequency at $k_\perp=0$ [Fig. 6(b)]. There is no Goldstone mode in the unflopped state. As noted earlier, the spin waves in the unflopped state have the character of standing-wave resonances in the constituent films. Because the resonant frequencies of the ferromagnetic and antiferromagnetic media differ substantially, a disturbance in one medium does not readily propagate through the neighboring film. The disturbance decays to zero in an exponential fashion into the neighboring constituents, as one of these modes is excited. The exponential "tails" which extend into neighboring films lead to interaction between modes localized in nearby films of similar character (say, between modes localized in adjacent ferromagnetic films), and this leads to dispersion in the superlattice eigenfrequencies, as the component of wave vector $k_\perp$ normal to the interfaces is varied. Because there are only four layers of nonresonant spins between adjacent resonant films, the magnitude of the dispersion, particularly of the lowest-frequency modes, can be appreciable.

As the Zeeman field is raised to approach the value required to induce a transition back to the unsymmetric spin-flop state, the lowest-frequency mode approaches zero frequency. This mode once again becomes the Goldstone mode of the system when the external field reaches the value required to induce a transition to the high-field unsymmetric spin-flop state [Fig. 6(c)].

When the Zeeman field reaches the critical value leading to a transition to the superlattice spin-flop state, the Goldstone mode becomes increasingly localized in the spin-flopped antiferromagnetic films. At the field strengths which place the system in the superlattice spin-flop state, the spins in the ferromagnetic films are nearly pinned along the direction of the field, and the large mismatch between the ferromagnetic and antiferromagnetic film resonance frequencies effectively cuts off communication between adjacent antiferromagnetic films. The Goldstone mode has zero frequency, is highly localized within the antiferromagnet, and no dispersion in $k_\perp$. To within our numerical accuracy, the dispersion cannot be resolved. This flat, zero-frequency branch would have finite frequency as a consequence if dipolar couplings were present.

In addition, the frequency of the $k_\perp=0$ second spin-wave branch [labeled Ω_2 in Fig. 5(a), where it is shown at a lower value of the external field] decreases to zero as the magnetic field approaches the transition to the paramagnetic state. This mode, which is localized in the antiferromagnetic films, is then the soft mode associated with the second-order phase transition from the unsymmetric to the superlattice spin-flop state.

When J_I takes the larger value $J_I=1.5$, the condition for the existence of the unflopped phase ($J_I \leq 0.79 J_{\rm FM}$) of the superlattice is not satisfied, and the Goldstone mode is present in all phases below the fully-aligned paramagnetic phase. We show the Goldstone mode in the unsymmetric phase in Fig. 6(e), at a value of the field H_0 slightly below that required to induce a transition to the superlattice spin-flop state. Once again, in the proximity of a highly symmetric state, we see an increase in the quadratic variation of the mode for small values of $k_\perp$, over that present at lower values of H_0 [cf. Ω_1 in Fig. 5(b)]. Again Ω_2 plays the role of the soft mode in the second-order transition to the superlattice spin-flop state.

In Fig. 6(e) we show the flat dispersion curve of the Goldstone mode in the superlattice spin-flop state. As in the case when $J_1=0.5$, the Goldstone mode is again localized in the antiferromagnetic film, but now with appreciable spin motion in the first layer of spins in the neighboring ferromagnetic films.

At higher fields, an increasing number of low-frequency spin-wave dispersion curves show no dispersion. These modes become strongly localized in the spin-flopped antiferromagnetic films because the spins in the ferromagnetic films are pinned along the direction of the Zeeman field H_0. Consequently, these modes do not readily propagate through the ferromagnetic regions, and we realize an analogue of the standing-spin-wave resonances of the unflopped phase of the superlattice structure. We comment here that those high-frequency modes in the spin-flop phases, which are approximately localized to the interfaces, continue to show appreciable dispersion

in the high-field region.

This summarizes our studies of the spin waves in the various phases of the superlattice structure. We see that the second-order phase transition from the unsymmetric to the superlattice spin-flop state has a soft mode associated with it, and we find that in the low-symmetry phases, various low- and high-frequency spin-wave branches have the character of collective excitations of the entire structure, as opposed to waves approximately localized to one constituent.

IV. THE INFRARED ABSORPTION SPECTRUM OF THE SUPERLATTICE

In this section we present the results of our study of the microwave or near-infrared absorption spectrum of the model superlattice structures discussed in this paper. As in Sec. III, we refer the reader to our previous paper[6] on the magnetic properties of superlattice structures (Appendix B), for a description of the details of the calculation of the absorption spectrum.

We calculate the response of the superlattice to an externally applied, time-dependent magnetic field taken parallel to the x axis. Thus, at lattice site l, the spin is driven by the field

$$\mathbf{h}(l)=h_x(l)\cos(\Omega t)\hat{\mathbf{x}}=\tfrac{1}{2}h_x(l)(e^{i\Omega t}+e^{-i\Omega t})\hat{\mathbf{x}}\ , \qquad (4.1)$$

which introduces into the Hamiltonian the interaction term

$$V=-\tfrac{1}{2}\sum_l h_x(l)\cos(\Omega t)[S_+(l,t)+S_-(l,t)]\ .$$

It is a straightforward matter to generalize the formalism presented in our previous paper to accommodate a unit cell in which there are two spins, with spin angles θ and θ', per sheet of spins. We do this simply by rewriting the eigenvector $\mathbf{S}'$ of the present system:

$$\mathbf{S}'=\begin{bmatrix} S'_+(\theta) \\ S'_+(\theta') \\ S'_-(\theta) \\ S'_-(\theta') \end{bmatrix} \rightarrow \mathbf{S}'=\begin{bmatrix} S'_+ \\ S'_- \end{bmatrix}\ .$$

With this regrouping of the elements in the eigenvector, the form of the resulting matrix problem is identical to that of our earlier work. Thus, we may use Eq. B26 (in Ref. 6) for the power absorbed by the (110) superlattice, provided we include in the sums the contributions of the two nonequivalent spins in each spin sheet. We turn now to the results of this study.

In Fig. 7, we show the calculated absorption spectrum for the various ground-state spin configurations of the superlattice with strong interface coupling, $J_I=1.5$. The units of frequency are such that the zero-field bulk antiferromagnetic resonance frequency is unity. In Fig. 7(a), we show the absorption spectrum for the case when the superlattice is in the unsymmetric state. The high-frequency feature is a resonance associated with the

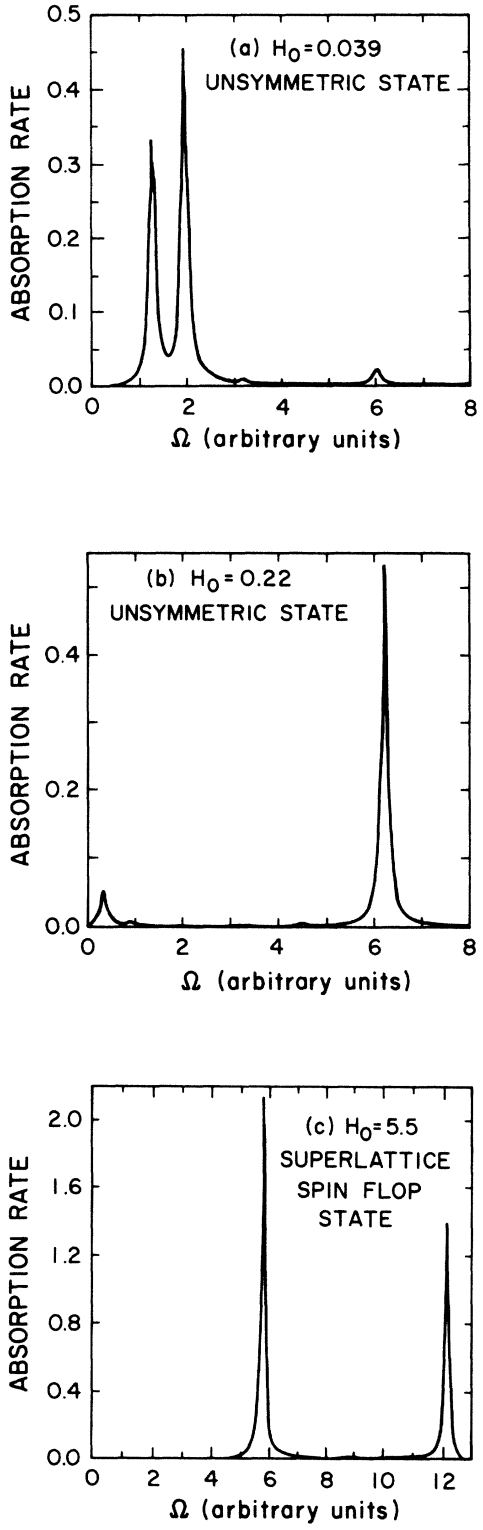

FIG. 7. For $N_{FM}=N_{AFM}=4$ and $J_I=1.5$, we show the infrared absorption spectrum, in arbitrary units, for several values of the external Zeeman field. In (a), the field has a low value in the unsymmetric state, in (b) it lies just a bit below that required to induce the superlattice spin-flop state, and in (c) it is large enough for the system to be within the superlattice spin-flop state. The units of frequency are the same as those used in Figs. 5 and 6. The magnetic field is measured in units of $(2H_EH_A)^{1/2}$.

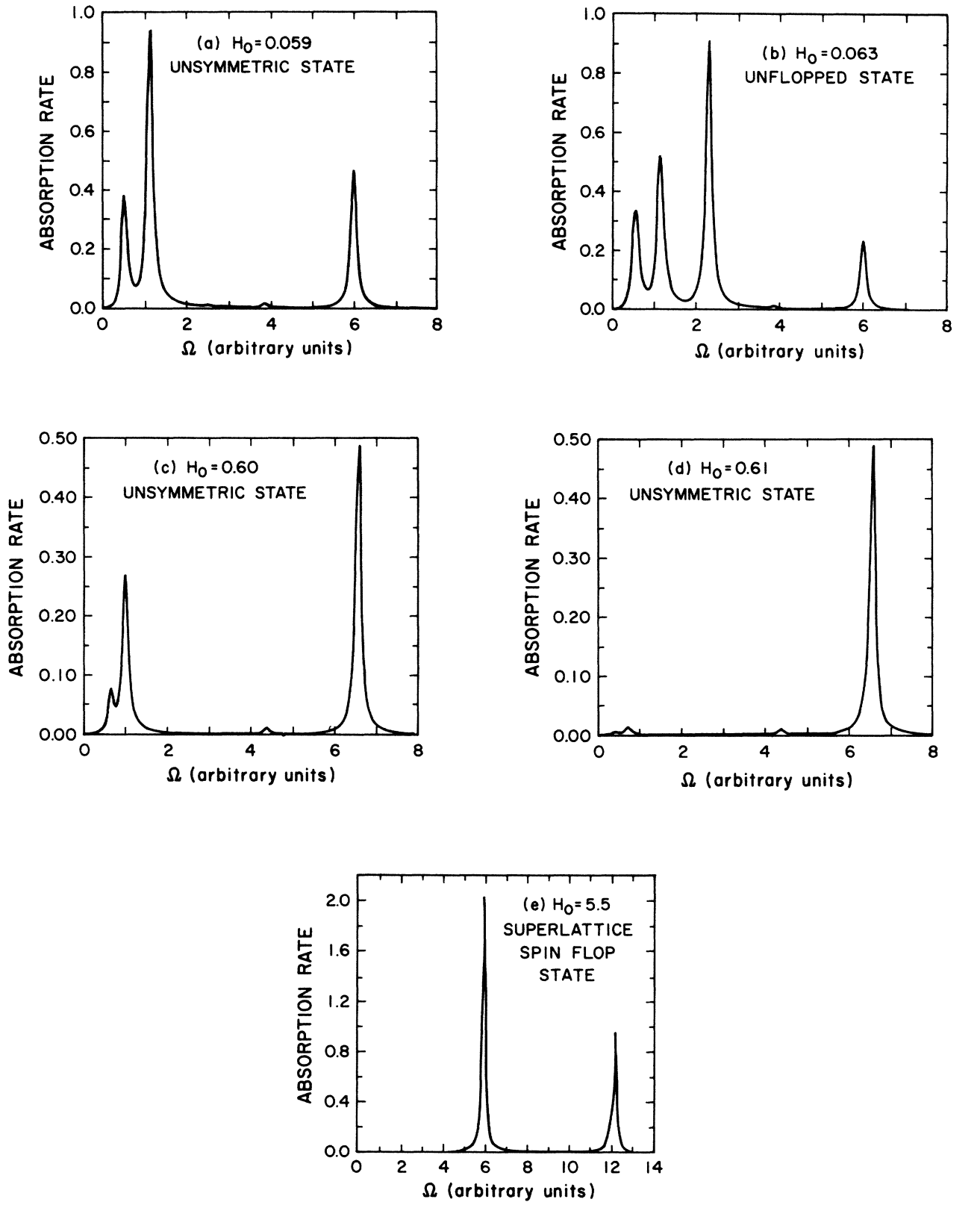

FIG. 8. We show the infrared absorption spectrum, in arbitrary units, for the case $N_{FM}=N_{AFM}=4$ and $J_I=0.5$, for various values of the field. In (a), the Zeeman field is just a bit below that required to induce the unflopped state, in (b) and (c) it lies within the range of the unflopped and unsymmetric states, respectively; in (d) the field lies just below that required to induce the superlattice spin-flop state, and in (e) it is large enough for the system to be within the superlattice spin-flop state. The units of frequency and field are the same as those used in Fig. 7.

highest-frequency mode (Ω_{16}) localized in the interfaces between the ferromagnetic and antiferromagnetic films. This resonance associated with the highest-frequency interface mode is present in the absorption spectrum throughout the entire range of the magnetic field, below the paramagnetic state.

The two strong, low-frequency features in the spectrum are modes localized in the antiferromagnet. The lower of these two features, a mode strongly localized in the antiferromagnet, occurs at the frequency slightly above that of the bulk antiferromagnetic resonance frequency. This mode is shifted above the bulk value by the effect of the surrounding ferromagnetic films, which act to "pin" the antiferromagnetic spins near the interface, thereby enhancing the exchange energy of this mode. The higher of the two low-frequency features is also a mode localized in the antiferromagnet; however, in this mode the amplitude of the spin motion in the first layer of spins in the neighboring ferromagnetic films is appreciable. This antiferromagnetic mode leaks into the ferromagnetic regions via those ferromagnetic interface spins which are nearly aligned with the antiferromagnetic interface spins (see Fig. 1). This alignment results in an even greater enhancement of the exchange energy, and a greater shift above the bulk resonance frequency, of this mode than was observed for the strongly localized antiferromagnetic mode. The remaining weak feature in the absorption spectrum is an "excited state" of the antiferromagnetic film.

Figure 7(b) shows the absorption spectrum of the superlattice in the unsymmetric state, at a value of the Zeeman field H_0 just below that required to drive the low-field ground state unstable. We see that the intensity of the high-frequency interface feature has increased, while that of both low-frequency features has decreased. In addition, the two antiferromagnetic features are shifted to lower frequencies. The lowest mode, still strongly localized in the antiferromagnetic, is the one which softens. As H_0 increases, this mode, labeled Ω_2 in Fig. 5(b), becomes the "soft mode" associated with the second-order magnetic-field-induced phase transition to the superlattice spin-flop state.

In the superlattice spin-flop state, we find two features in the absorption spectrum. For a particular choice of field, this spectrum is illustrated in Fig. 7(c). The high-frequency feature is the absorption associated with the highest-frequency interface mode, Ω_{16}. The low-frequency feature is the mode strongly localized in the antiferromagnet, and this feature has a frequency which increases linearly with H_0.

We now turn to the calculated absorption spectrum of the superlattice for the case when $J_I=0.5$. This spectrum is given in Fig. 8 for the various ground-state spin configurations of the superlattice structure.

Figure 8(a) shows the low-field absorption spectrum, at a value of the Zeeman field just below that required to induce transition from the unsymmetric to the unflopped state. Again, the high-field feature is localized in the interfaces, and the weak intermediate features are excited states of the antiferromagnet. The low-field features are localized in the antiferromagnetic films.

In Fig. 8(b) we show the absorption spectrum at a value of the field just above the critical field of the transition to the unflopped state. We see the appearance of a new strong resonance localized in the antiferromagnet. Recall that in this phase the spin waves have the character of standing-wave resonances and each mode is localized in one or the other constituent. The first and third low-frequency features are the low- and high-frequency partners of the antiferromagnetic resonance doublet, split by interaction with the Zeeman field and exchange coupling between the antiferromagnet and the neighboring ferromagnetic films. The second strong low-frequency feature is a mode localized in the ferromagnetic films. The weak high-frequency features are excited states of the ferromagnet.

We show the absorption spectrum of the superlattice in the high-field unsymmetric state, in Fig. 8(c). Note the disappearance of the third strong low-frequency feature present in Fig. 8(b). The spectrum in Fig. 8(c) is qualitatively similar to that in Fig. 7(a). Again, the first low-frequency feature is strongly localized in the antiferromagnetic films, while the second feature involves antiferromagnetic spins and the first layer of ferromagnetic spins. Again, the lowest-frequency feature softens as the value of the field approaches that of the superlattice spin-flop transition [Fig. 8(d)].

In the superlattice spin-flop state for the case when $J_I=0.5$, we again find two features in the absorption spectrum. These are illustrated for a particular choice of field in Fig. 8(c). This spectrum is analogous to that in Fig. 7(c), for the case when $J_I=1.5$.

V. CONCLUDING REMARKS

This paper has been devoted to a theoretical study of a model of a superlattice formed by alternating layers of ferromagnetic and antiferromagnetic materials, in which the antiferromagnetic constituent is composed of mixed-spin sheets of spin. This work is a continuation of our study of similar superlattice structures, in which the antiferromagnetic material is composed of sheets of spin within which the moments are aligned ferromagnetically.

The geometry explored in this paper leads to very different behavior of the macroscopic properties of the resulting material, such as the phase diagram and the infrared absorption spectrum. A striking feature is the spin pattern of the ground state for low values of an externally applied magnetic field, including zero field. This low-field ground state has spins canted to minimize total exchange energy at the interface in contrast to the unflopped low-field ground state of the superlattice structures considered in our previous work, as well as that of the bulk antiferromagnetic. Another new feature is the presence of strongly localized interface modes.

We find that the macroscopic properties of magnetic superlattice systems are influenced strongly by the microscopic details of the underlying structure.

ACKNOWLEDGMENT

This research is supported by the Army Research Office, through Grant No. PO426620.

[1]M. B. Stearns, C. H. Lee, and S. P. Vernon, in Proceedings of the International Conference on Magnetism, San Francisco, 1985 (unpublished).
[2]C. Schlenker, S. S. P. Parkin, J. C. Scott, and K. Howard, in Proceedings of the International Conference on Magnetism, San Francisco, 1985 (unpublished).
[3]J. C. Scott, J. Appl. Phys. **57**, 3681 (1985).
[4]C. Vettier, D. B. McWhan, E. M. Gyorgy, J. Kwo, B. M. Buntshuh, and B. W. Batterman, Phys. Rev. Lett. **56**, 757 (1986).
[5]L. L. Hinchey and D. L. Mills, J. Appl. Phys. **57**, 3687 (1985).
[6]L. L. Hinchey and D. L. Mills, Phys. Rev. B **33**, 3329 (1986).
[7]A. Kueny, M. R. Khan, I. K. Schuller, and M. Grimsditch, Phys. Rev. B **29**, 2879 (1984).
[8]R. Damon and J. Eshbach, J. Phys. Chem. Solids **19**, 308 (1961).
[9]R. E. Camley, T. S. Rahman, and D. L. Mills, Phys. Rev. B **27**, 261 (1983).
[10]P. Gruenberg and K. Mika, Phys. Rev. B **27**, 2955 (1983).
[11]K. Mika and P. Gruenberg, Phys. Rev. B **31**, 4465 (1985).
[12]In practice, the spins in the ferromagnetic films will usually align themselves parallel to the interfaces to avoid generating demagnetizing fields of dipolar origin. Thus we confine our attention to spin configurations of the superlattice for which all spins in each (110) plane are aligned parallel to the interfaces.
[13]In contrast, the ground-state spin arrangement of the (100) superlattice is different for N_{AFM} odd than for N_{AFM} even. Because the antiferromagnet consists of ferromagnetically aligned sheets of spins with ferromagnetic alignment alternately up and down, the moments in adjacent ferromagnetic films may alternate up and down (N_{AFM} even), or have the same orientation (N_{AFM} odd).
[14]In the absence of dipolar coupling, the Hamiltonian is invariant under rotations of the spin configuration about the axis, so we may choose to confine the spins to any plane we wish. As remarked in Ref. 12, in the presence of the dipolar interactions, in those spin configurations where a transverse moment is present, the spins will lie in the plane parallel to the interfaces.
[15]F. B. Anderson and H. B. Callen, Phys. Rev. **136**, 1068 (1964).